Stability Analysis of Three-Dimensional Colloidal Domains: Quadratic Fluctuations†

Jianlan Wu and Jianshu Cao*

Department of Chemistry, Massachusetts Institute of Technology, Cambridge, Massachusetts 02139

Received: May 10, 2005; In Final Form: July 11, 2005

Three-dimensional domain patterns can self-assemble in a charged colloidal suspension with competing short-range attraction and long-range Yukawa repulsion. Following the investigation of the ground-state domain shapes in our previous paper, we study the stability of isolated spherical, cylindrical, and lamellar domains with respect to shape fluctuations on boundaries. In the framework of the continuum model, we expand the free energy variation to quadratic terms under the constraint of constant volume. For the three shapes (sphere, cylinder, and lamella) discussed, domains with equilibrium sizes are stable with respect to shape fluctuations, and the stability of domains decreases as the spatial symmetry decreases.

I. Introduction

In many self-assembly systems,[1−8] the formation of domain patterns can be explained successfully by the competing interactions on different length scales.[9−19] In a previous paper,[20] we studied ground-state domains in charged colloidal suspensions based on an effective pairwise colloid−colloid interaction with a short-range attraction and a long-range repulsion. The short-range attraction can be modeled by a square-well potential with depth ϵ and the range in $(\sigma, \lambda\sigma)$, where σ is the diameter of colloidal particles. By adjusting parameters ϵ and λ, the square-well form can provide qualitatively the same results as other potential forms.[21,22] Because of the nature of the screened electrostatics in charged colloids, the long-range repulsion is described by the Yukawa potential,[23,24] which is different from the dipole−dipole interaction in two-dimensional (2D) lipid systems.[15,25−29] The repulsion strength is denoted by A, and the screening length is represented by ζ. To be consistent with ref 20, all the length variables in the paper are dimensionless in units of ζ. The effective potential between two colloidal particles distanced by r is given by

$$u(r)=\begin{cases}\infty & r \le \sigma \\ -\epsilon & \sigma < r \le \lambda\sigma \\ u_{\mathrm{Y}}(r) = A\zeta r^{-1}\, \mathrm{e}^{-r/\zeta} & r > \lambda\sigma\end{cases} \qquad (1)$$

where the hard-core repulsion is included, since colloidal particles cannot penetrate each other.

Although eq 1 is a well-defined pairwise potential for studying thermodynamic properties of domains in charged colloidal suspensions, analytical calculations are complicated in providing useful predictions. An alternative approach is to adopt the continuum model where the summation over particles is approximated by the integral over space weighted by density. For example, a mean-field continuum model has been used to study the block copolymer by Leibler[9] and extended by Ohta and Kawasaki.[10] At low temperatures, boundaries separating domains and dispersing medium are sharp, and the continuum model can be further simplified by neglecting the colloidal density fluctuations except for abrupt changes across boundaries.[15,25−29] On the basis of this simplified model, we investigated ground-state colloidal domains in spherical, cylindrical, and lamellar shapes in ref 20. The most stable domain shape and structure are determined by the global minimum of the energy density, and a phase diagram of the shape transformation is obtained.[20]

A complete thermodynamic study of domains requires the stability analysis with respect to thermal fluctuations, which assist the evolution from a homogeneous mixture to spatially modulated phases and induce the shape transformation of domains. At high temperatures, thermal fluctuations can be described by density fluctuations of colloidal particles,[16,17,30] whereas at low temperatures, thermal fluctuations can be effectively described by shape fluctuations on sharp boundaries separating domains and dispersing medium.[15,25−33] These two descriptions are both widely applied in the literature. In this paper, we focus on the low temperature and density regime where each domain can be treated as an isolated system. Our analysis of the domain stability is based on the evaluation of the free energy variation with respect to small shape fluctuations. When the free energy variation δF is positive, the domain has a restoring force to recover its original shape so that it is a (meta)stable state. Otherwise, the reference shape is unstable, and fluctuations induce spontaneous and irreversible transformations. For the reference shape, the sign of δF determines stable and unstable regimes with respect to shape fluctuations. To obtain δF, we follow the theoretical method used by Deutch and Low in 2D lipid systems:[27] Shape fluctuations are expanded in successive orders by fixing the domain volume and are then used to calculated the free energy variation within the quadratic approximation.

II. Continuum Model

The system we study is a colloidal suspension with a fixed number density, $\rho_0 = N/V_{\mathrm{tot}}$, where N is the total number of colloidal particles and V_{tot} is the volume of system. With a continuous colloidal number density $\rho(\vec{r}) = \sum_{i=1}^{N}\delta(\vec{r} - \vec{r}_i)$, the sum over all the colloidal particles becomes an integral with the weight $\rho(\vec{r})$, i.e., $\sum_{i=1}^{N} f_i = \int \mathrm{d}\vec{r}\ \rho(\vec{r})\, f(\vec{r})$, where $\vec{r}_i$ is the position of the ith particle and f is an arbitrary function. At high temperatures, the system is homogeneous and $\rho(\vec{r})$ is a uniform function with the constant value of ρ_0. Below a critical

† Part of the special issue "Irwin Oppenheim Festschrift".

* Email: jianshu@mit.edu.

10.1021/jp0524431 CCC: $30.25
Published on Web 09/01/2005

temperature, colloidal particles aggregate into domains through a self-assembly process, and $\rho(\vec{r})$ becomes a periodical function in space. At low temperatures, domains and dispersing medium are separated by sharp boundaries, across which $\rho(\vec{r})$ jumps from a nonzero value to zero. Assuming that colloidal particles are uniformly distributed inside domains, the density function is reduced to

$$\rho(\vec{r}) = \begin{cases} \rho_1 & \text{inside domains} \\ \rho_2 & \text{outside domains} \end{cases} \tag{2}$$

where ρ_2 is set to be zero in this paper for convenience. The neglect of density fluctuations in eq 2 is acceptable at low temperatures, since shape fluctuations are dominant as discussed in the Introduction.

In the mean-field framework, the short-range attraction contributes to bulk adhesion and surface free energy. The bulk adhesion, is expressed as $F_A = \int d\vec{r}\ \rho(\vec{r})\ f_A(\vec{r})$, where $f_A(\vec{r})$ is the adhesive free energy density. Consistent with the simplification for the density function, $f_A(\vec{r})$ is approximated by its average value, $f_A = -n_c\epsilon/2$, where n_c is the average contact number per particle. Since the bulk adhesion in a unit system volume, $F_A/V = -\rho_0 v_0 n_c\epsilon/2$, is a shape-independent constant, F_A does not contribute to the shape transformation and will be neglected. For a single domain Γ with surface area S_d, its surface free energy is given by $F_S(\Gamma) = \oint_{S_d} d\vec{r}\ \gamma(\vec{r}) \approx \gamma S_d$. Although the surface tension γ is a shape-dependent function in general, we apply the zeroth-order approximation and consider γ as a constant. As an implicit function of temperature, the surface tension decreases as temperature increases.

The integrated contribution of the long-range Yukawa repulsion to free energy can be simplified to

$$\sum_{i<j=1}^{N} u_Y(r_{ij}) = \sum_{m=1}^{N_d} F_Y^{(1)}(m) + \sum_{m<n=1}^{N_d} F_Y^{(2)}(m,n) \tag{3}$$

where $r_{ij} = |\vec{r}_i - \vec{r}_j|$ and N_d is the total number of domains. In the above equation, $F_Y^{(1)}(m)$ is the intradomain repulsive free energy for domain Γ_m

$$F_Y^{(1)}(m) = \int_{\Gamma_m} d\vec{r}_1 \int_{\Gamma_m} d\vec{r}_2 \frac{\rho(\vec{r}_1)\,\rho(\vec{r}_2)}{2} u_Y(|\vec{r}_1 - \vec{r}_2|) \tag{4a}$$

whereas $F_Y^{(2)}(m, n)$ is the interdomain repulsive free energy between two domains, Γ_m and Γ_n

$$F_Y^{(2)}(m, n) = \int_{\Gamma_m} d\vec{r}_1 \int_{\Gamma_n} d\vec{r}_2\, \rho(\vec{r}_1)\,\rho(\vec{r}_2)\, u_Y(|\vec{r}_1 - \vec{r}_2|) \tag{4b}$$

In the low-density limit, the distance between a pair of domains is much larger than the characteristic domain size, so that each domain can be treated as an isolated system, and the collective contribution of $F_Y^{(2)}(m, n)$ is ignored in the lowest-order approximation. The resulting effective free energy for a single domain is written as

$$F \approx F_S + F_Y^{(1)} \tag{5}$$

In a more rigorous manner, the sum on the right-hand side of eq 5 should be treated as energy instead of free energy. Since the entropic effects can be partially included by the temperature-dependent surface tension γ, and the configurational randomness of domains is omitted for the case of isolated domains, we consider eq 5 as a good approximation for the free energy. In the remainder of this paper, we will calculate the variation of F with respect to shape fluctuations for spherical, cylindrical, and lamellar domains.

III. Spherical Domains

As shown in our previous paper,[20] spherical domains are energetically preferred in the low-density and weak attraction limits. In this section, we analyze the stability of spherical domains and study the shape transformation driven by spherical harmonic shape fluctuations.

We first introduce a small fluctuation $\delta R(\Omega)$ for a reference spherical domain with radius R. Following Deutch and Low's approach,[27] we expand the shape fluctuation in successive orders

$$\delta R(\Omega) = \delta R_0(\Omega) + \delta R_1(\Omega) + \cdots \tag{6}$$

where $|\delta R_0| \gg |\delta R_1| \gg \cdots$. The same expansion will be applied for the stability analysis of cylindrical domains in the next section. According to this shape fluctuation, the domain volume formally changes from $V_{d,0} = 4\pi R^3/3$ to

$$V_d = \frac{1}{3}\oint d\Omega [R + \delta R(\Omega)]^3$$
$$\approx V_{d,0} + R^3 \oint d\Omega \left[\frac{\delta R(\Omega)}{R} + \frac{\delta R^2(\Omega)}{R^2} + O\left(\frac{\delta R^3(\Omega)}{R^3}\right)\right] \tag{7}$$

where $\oint d\Omega = \int_0^{\pi} \sin\theta\, d\theta \int_0^{2\pi} d\phi$ is the integral over the solid angle Ω. The volume of a stable domain remains the same with respect to fluctuations, i.e., $V_d = V_{d,0}$. On the basis of this constraint, the leading-order fluctuation satisfies $\oint d\Omega\ \delta R_0(\Omega) = 0$, and the next order satisfies $\delta R_1(\Omega) = -\delta R_0^2(\Omega)/R$. Using spherical harmonics $Y_{lm}(\Omega)$, we expand $\delta R_0(\Omega)$ as

$$\delta R_0(\Omega) = \sum_{l=1}^{\infty} \delta R_0(l, \Omega) = \sum_{l=1}^{\infty} \sum_{m=-l}^{l} c_{lm} Y_{lm}(\Omega) \tag{8}$$

where $c_{l,-m} = (-1)^m c_{lm}^*$ is required, since $\delta R_0(\Omega)$ is real.

Next, we calculate the variation of the free energy F with respect to the shape fluctuation $\delta R(\Omega)$. In the low-density limit, the free energy of a colloidal domain is approximated as a sum of the surface free energy F_S and intradomain repulsion $F_Y^{(1)}$. With a constant surface tension γ, the variation of F_S only depends on the change of surface area S_d. Similar to eq 7, the surface area difference is truncated to quadratic terms

$$\delta S_d = \oint d\Omega \{[R + \delta R(\Omega)] \sqrt{[R(\Omega) + \delta R(\Omega)]^2 + |\nabla_{\vec{\Omega}}\, \delta R(\Omega)|^2} - R^2\}$$
$$\approx \oint d\Omega [|\nabla_{\vec{\Omega}}\, \delta R_0(\Omega)|^2 - \delta R^2{}_0(\Omega)] \tag{9}$$

where $\nabla_{\vec{\Omega}}$ is the gradient operator for the solid angle Ω, $\nabla_{\vec{\Omega}} = \partial_\theta\, \hat{e}_\theta + (\sin\theta)^{-1}\partial_\phi \hat{e}_\phi$, and $\{\hat{e}_r, \hat{e}_\theta, \hat{e}_\phi\}$ are unit vectors in spherical coordinates. The relation, $\delta R_1(\Omega) = -\delta R^2{}_0(\Omega)/R$, is applied to derive eq 9. Following the expansion in eq 8 and the spherical harmonic differential equation, $\nabla_{\vec{\Omega}}^2 Y_{lm}(\Omega) = -l(l+1)Y_{lm}(\Omega)$, we obtain the surface free energy variation

$$\delta F_S = \gamma \delta S_d = \gamma \sum_{l=1}^{\infty} \sum_{m=-l}^{l} [l(l+1) - 1]|\, c_{lm}|^2 \tag{10}$$

In spherical coordinates, the intradomain repulsion is explicitly written as

$$F_{\mathrm{Y}}^{(1)} = \frac{\rho^2{}_1}{2} \oint \mathrm{d}\Omega_1 \oint \mathrm{d}\Omega_2 \int \mathrm{d}r_1 \int \mathrm{d}r_2 r^2{}_1 r^2{}_2 u_{\mathrm{Y}}(r_{12}) \quad (11)$$

where the distance between two vectors $\vec{r}_1$ and $\vec{r}_2$ is given by $r_{12} = |\vec{r}_1 - \vec{r}_2| = (r_1^2 + r_2^2 - 2r_1 r_2 \cos\chi)^{1/2}$, and χ is the angle between these two vectors, $\cos\chi = \cos\theta_1 \cos\theta_2 + \sin\theta_1 \sin\theta_2 \cos(\phi_1 - \phi_2)$. After a straightforward but tedious derivation, the quadratic truncation of the intradomain repulsion variation is given by

$$\delta F_{\mathrm{Y}}^{(1)} = \frac{R^4 \rho^2{}_1}{2} \oint \mathrm{d}\Omega_1 \oint \mathrm{d}\Omega_2 \, \delta R_0(\Omega_1) \, \delta R_0(\Omega_2) u_{\mathrm{Y}}(|R\hat{e}_{r_1} - R\hat{e}_{r_2}|) + \frac{R^2 \rho^2{}_1}{2} \oint \mathrm{d}\Omega_1 \oint \mathrm{d}\Omega_2 \int_0^R \mathrm{d}r_1 r^2{}_1 \, \delta R^2{}_0(\Omega_2) [\hat{e}_{r_2} \cdot \nabla_{\vec{r}_2} u_{\mathrm{Y}}(|\vec{r}_1 - R\hat{e}_{r_2}|)] \quad (12)$$

where the gradient operator for vector $\vec{r}$ is $\nabla_{\vec{r}} = \partial_r \hat{e}_r + r^{-1}\nabla_{\vec{\Omega}}$ in spherical coordinates. We apply the spherical harmonic expansion and simplify eq 12 to

$$\delta F_{\mathrm{Y}}^{(1)} = \pi R^4 \rho^2{}_1 A \sum_{l=1}^{\infty} \sum_{m=-l}^{l} |c_{lm}|^2 [g_l(R, R) - g_1(R, R)] \quad (13)$$

where $g_l(r_1, r_2)$ is defined using the lth-order Legendre polynomial $P_l(\cos\chi)$ as

$$g_l(r_1, r_2) = A^{-1} \int_0^{\pi} \mathrm{d}\chi \sin\chi P_l(\cos\chi) u_{\mathrm{Y}}(r_{12}) \quad (14)$$

The details of this derivation are shown in Appendix A. The free energy variation for a spherical domain is the sum of eqs 10 and 13.

As discussed in section I, the sign of the free energy variation determines the stable ($\delta F > 0$) and unstable ($\delta F < 0$) regimes with respect to a given shape fluctuation. Since the free energy variation for a spherical domain is diagonalized in the basis of $Y_{lm}(\Omega)$, we focus on spherical harmonic shape fluctuations. Several examples are shown in Figure 1. With respect to the lth-order mode, $\delta R_0(l, \Omega) = \sum_{m=-l}^{l} c_{lm} Y_{lm}(\Omega)$, the critically stable radius R_l is determined by

$$\alpha[l(l+1) - 1] + R_l^4 [g_l(R_l, R_l) - g_1(R_l, R_l)] = 0 \quad (15)$$

where the effective attraction−repulsion ratio, $\alpha = \gamma/\pi\rho_1^2 A\zeta^4$, is introduced in ref 20. A direct result of eq 15 is that spherical domains are always stable with respect to the first-order shape fluctuation mode ($l = 1$). Here, we recall the equilibrium spherical radius R_{eq} determined by[20]

$$\frac{\mathrm{d}F}{\mathrm{d}R_{\mathrm{eq}}} \propto (1 - \alpha)R_{\mathrm{eq}}^2 - 3 + (2R_{\mathrm{eq}}^3 + 5R_{\mathrm{eq}}^2 + 6R_{\mathrm{eq}} + 3)\mathrm{e}^{-2R_{\mathrm{eq}}} = 0 \quad (16)$$

For conciseness, the notation of "equilibrium" is introduced loosely throughout this paper to represent the optimal state for a given shape instead of the state with the global minimum free energy density. In addition, the symbol R_{eq} is introduced, since the original one, R_m, in ref 20 will be used as the mth-order critical radius for cylindrical domains in this paper. In Figure 2, ratios between critical and equilibrium radii are plotted as functions of α for the first three important fluctuation modes. With respect to the lth-order shape fluctuation, spherical domains are stable below the curve of $R_l(\alpha)/R_{\mathrm{eq}}(\alpha)$, whereas they are unstable above this curve. Since the value of R_l is at least twice the equilibrium radius, spherical domains in equilibrium are always stable with respect to shape fluctuations in the quadratic approximation. In the weak attraction limit ($\alpha \to 0$), the critical

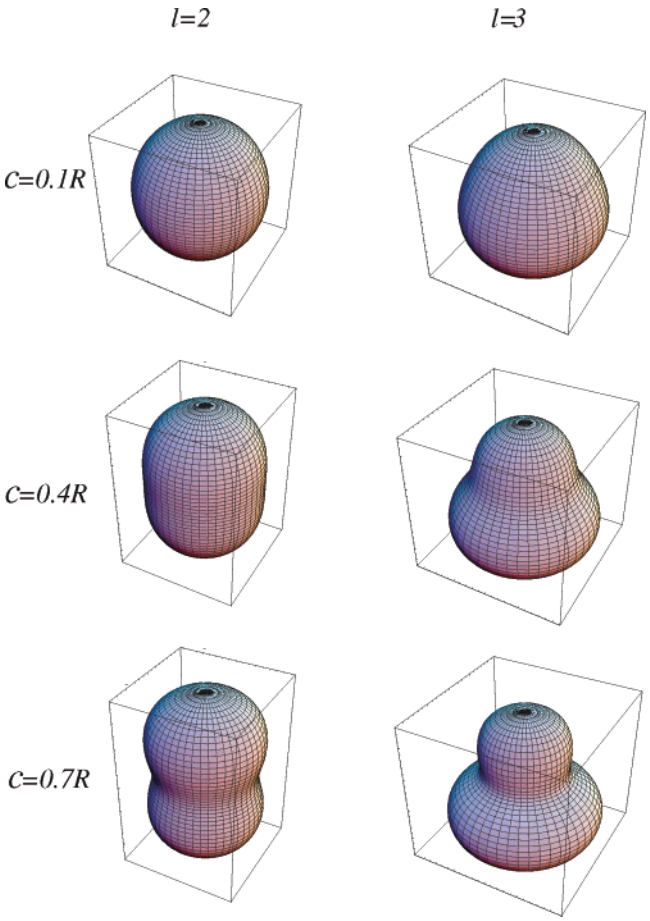

Figure 1. Examples of spherical harmonic shape fluctuations with $\delta R_0 = cY_{l0}(\Omega)$. Three figures on the left side correspond to $l = 2$, and the other three on the right side correspond to $l = 3$. For figures in the same row, their values of c are the same and shown on the left.

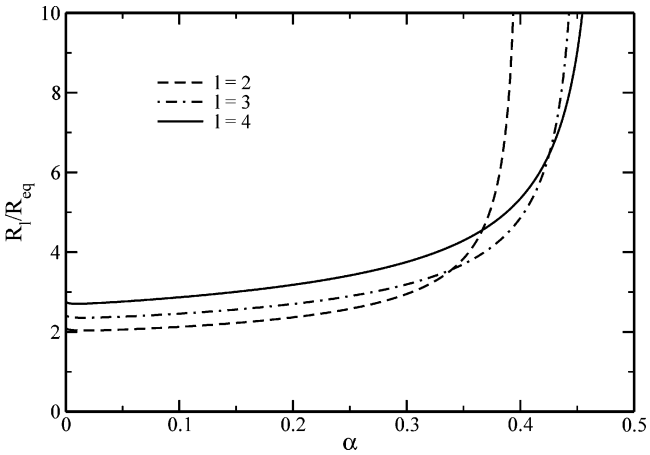

Figure 2. The stability curves for spherical domains. With respect to the $l(\geq 2)$th order spherical harmonic fluctuation mode, spheres are stable below the corresponding stability curve, whereas they are unstable above this curve.

radius R_l is an increasing function of l, so that the second-order shape fluctuation ($l = 2$) is the most important mode. Asymptotically, the ratio between critical and equilibrium radii is given by

$$\lim_{\alpha\to 0}\frac{R_l}{R_{eq}} = \left[\frac{2(2l+1)(l^2+l-1)}{5(l-1)}\right]^{1/3} \tag{17}$$

With the increase of attraction strength, the critical radius R_l quickly increases. Above a critical point, $\alpha_l = (l^2 + l - 2)/[2(l^2 + l - 1)]$, the lth-order radius approaches infinity, and the associated free energy variation is always positive. For $\alpha > \alpha_\infty$ ($=1/2$), all the spherical domains can resist shape fluctuations in the quadratic approximation. Although other shapes such as cylinders become more energetically favorable than spheres for $\alpha > 0.788$ as shown in Figure 4 of ref 20, the transformation from isolated spheres to cylinders cannot be spontaneously achieved by shape fluctuations.

IV. Cylindrical Domains

In comparison to spheres and lamellae, cylindrical domains are the most stable state for $0.788 < \alpha < 0.846$ in the low-density limit.[20] Shape fluctuations for cylinders can be separated into two categories: about the radius and along the azimuthal axis. In this section, we will investigate shape fluctuations about the radius. The azimuthal shape fluctuations will be discussed together with shape fluctuations for lamellae in the next section because of their spatial similarities.

Similar to the approach for spherical domains, we expand the shape fluctuation in the Fourier basis under the constraint of constant volume. For a cylindrical domain with radius R and azimuth length $L(\gg 1)$, a fluctuation $\delta R(\theta)$ about R formally changes the volume from $V_{d,0} = \pi R^2 L$ to

$$\begin{aligned} V_d &= \int_{-L/2}^{L/2} dz \int_{-\pi}^{\pi} d\theta \int_0^{R+\delta R(\theta)} dr r \\ &= V_{d,0} + R^2 L \oint d\theta \left[\frac{\delta R(\theta)}{R} + \frac{\delta R^2(\theta)}{2R^2}\right] \end{aligned} \tag{18}$$

where $\oint d\theta = \int_0^{2\pi} d\theta$. Following the successive expansion, $\delta R(\theta) = \delta R_0(\theta) + \delta R_1(\theta) + \cdots$, the constant volume constraint for stable domains requires that the leading-order fluctuation satisfies $\oint d\theta\, \delta R_0(\theta) = 0$ and the next order satisfies $\delta R_1(\theta) = -\delta R_0^2(\theta)/(2R)$. The leading-order fluctuation can be expanded in the Fourier basis as $\delta R_0(\theta) = \sum_{m\neq 0} c_m e^{im\theta}$, where $c_{-m} = c_m^*$ since $\delta R_0(\theta)$ is real.

Using shape fluctuations in the expansion form, we calculate the free energy variation. Truncated to quadratic terms, the change of surface area with respect to $\delta R(\theta)$ is given by

$$\begin{aligned} \delta S_d &\approx L \oint d\theta \{\sqrt{[R+\delta R(\theta)]^2 + [\partial_\theta (R+\delta R(\theta))]^2} - R\} \\ &\approx \frac{L}{2R}\oint d\theta [(\partial_\theta \delta R_0(\theta))^2 - \delta R^2{}_0(\theta)] \end{aligned} \tag{19}$$

where the relation $\delta R_1(\theta) = -\delta R^2{}_0(\theta)/(2R)$ is applied. The expansion of the surface free energy variation in in the Fourier basis is thus written as

$$\delta F_S = \gamma \delta S = \frac{2\pi\gamma L}{R}\sum_{m=1}^{\infty} |c_m|^2 (m^2 - 1) \tag{20}$$

In cylindrical coordinates $\{\hat{e}_{r_\perp}, \hat{e}_\theta, \hat{e}_z\}$, vectors are expressed as $\vec{r} = \vec{r}_\perp + z\hat{e}_z = r_\perp \hat{e}_{r_\perp} + z\hat{e}_z$, and the explicit form of intradomain repulsion for a cylindrical domain is

$$\begin{aligned} F_Y^{(1)} &= \frac{\rho_1^2}{2}\int_{-L/2}^{L/2} dz_1 \int_{-L/2}^{L/2} dz_2 \int d\vec{r}_{\perp 1} \int d\vec{r}_{\perp 2} \\ &\qquad u_Y\left(\sqrt{(z_1 - z_2)^2 + |\vec{r}_{\perp 1} - \vec{r}_{\perp 2}|^2}\right) \\ &= \rho_1^2 AL \int d\vec{r}_{\perp 1} \int d\vec{r}_{\perp 2} K_0(|\vec{r}_{\perp 1} - \vec{r}_{\perp 2}|) \quad \text{for } L \gg 1 \end{aligned} \tag{21}$$

To derive the equation above, an integral identity, $\int_0^\infty dz\, \exp(-\sqrt{z^2+t^2})/\sqrt{z^2+t^2} = K_0(|t|)$, is applied, where $K_m(t)$ is the mth-order modified Bessel function of the second kind. With respect to $\delta R(\theta)$, we obtain the quadratic truncation for the intradomain repulsion variation

$$\begin{aligned} \delta F_Y^{(1)} = &\\ &\rho_1^2 ALR^2 \oint d\theta_1 \oint d\theta_2\, \delta R_0(\theta_1)\, \delta R_0(\theta_2) K_0(|R\hat{e}_{r_{\perp 1}} - R\hat{e}_{r_{\perp 2}}|) + \\ &\qquad \rho^2{}_1 ALR \oint d\theta_2\, \delta R_0(\theta_2) \oint d\theta_1 \int_0^R r_{\perp 1}\, dr_{\perp 1} \\ &\qquad\qquad \partial_{r_{\perp 2}} K_0(|r_{\perp 1}\hat{e}_{r_{\perp 1}} - R\hat{e}_{r_{\perp 2}}|) \end{aligned} \tag{22}$$

To expand $\delta F_Y^{(1)}$ in the Fourier basis, we introduce the addition theorem for Bessel functions[34]

$$K_0(a|\vec{r}_{\perp 1} - \vec{r}_{\perp 2}|) = \sum_{m=-\infty}^{\infty} K_m(ar_{\perp >}) I_m(ar_{\perp <})\, e^{im(\theta_1 - \theta_2)} \tag{23}$$

where $I_m(t)$ is the mth-order modified Bessel function of the first kind, and $r_{\perp >}$ and $r_{\perp <}$ denote the larger and smaller of $r_{\perp 1}$ and $r_{\perp 2}$, respectively. Substituting eq 23 into eq 22, the intradomain repulsion variation is given by

$$\delta F_Y^{(1)} = 2(2\pi)^2 \rho_1^2 ALR^2 \sum_{m=1}^{\infty} |c_m|^2 [K_m(R) I_m(R) - K_1(R) I_1(R)] \tag{24}$$

As a sum of eqs 20 and 24, the free energy variation for a cylindrical domain is diagonalized in the Fourier basis so that we will concentrate on harmonic shape fluctuations. Examples in Figure 3 show that an original cylindrical domain can evolve into m subdomains induced by the mth-order fluctuation mode, $\delta R_0(m, \theta) = c_m e^{im\theta} + c_m^* e^{-im\theta}$. Since the stability of domains is determined by the sign of δF, the mth-order critically stable radius R_m with respect to $\delta R_0(m, \theta)$ is given by

$$\frac{\alpha}{4R_m^3}(m^2 - 1) + K_m(R_m) I_m(R_m) - K_1(R_m) I_1(R_m) = 0 \tag{25}$$

The equation above shows that cylindrical domains remain marginally stable with respect to the first-order mode ($m = 1$). To discuss higher-order fluctuation modes, we recall the equilibrium cylindrical radius R_{eq}[20]

$$\frac{dF}{dR_{eq}} \propto 1 + \alpha R_{eq}^{-1} - 2K_1(R_{eq}) I_1(R_{eq}) = 0 \tag{26}$$

Here, we reemphasize that the equilibrium radius in the equation above is defined only for cylindrical domains without the consideration of other shapes. The results of $R_m(\alpha)/R_{eq}(\alpha)$ are plotted in Figure 4 as functions of the control parameter α. Similar to fluctuation modes for spheres, the mth-order shape

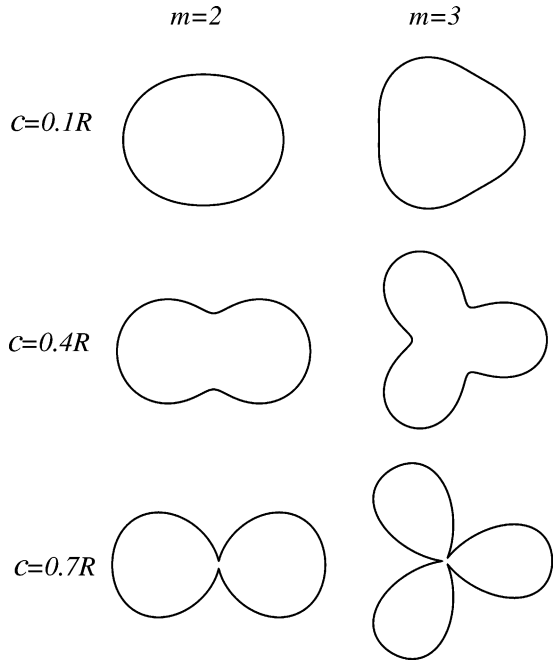

Figure 3. Examples of harmonic shape fluctuations with $\delta R_0 = c\cos(m\theta)$ projected in the *xy* plane. Three figures on the left side correspond to $m = 2$, and the other three on the right side correspond to $m = 3$. For shapes in the same row, their values of c are the same and shown on the left.

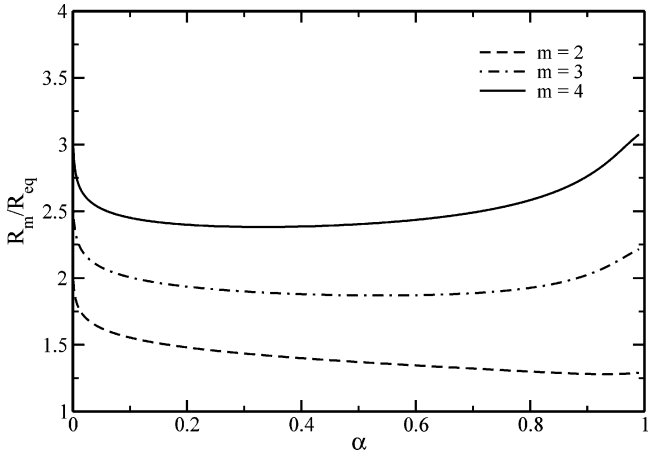

Figure 4. The stability curves for cylindrical domains. With respect to the $m(\geq 2)$th order fluctuation mode (see Figure 3), cylinders are stable below the corresponding stability curve, whereas they are unstable above this curve.

fluctuation can irreversibly distort cylinders in the regime above the curve of $R_m(\alpha)/R_{eq}(\alpha)$. Since R_m is greater than R_{eq} by at least 50%, equilibrium cylindrical domains are stable with respect to shape fluctuations in the quadratic approximation. As displayed in Figure 4, the critical radius R_m systematically increases as m increases, indicating that the second-order fluctuation ($m = 2$) is the most important mode for all the values of α.[28] In the weak attraction limit, eqs 25 and 26 can be asymptotically solved, resulting in

$$\lim_{\alpha\to 0}\frac{R_m}{R_{eq}} \approx \left[\frac{m(m+1)}{6}\log(\alpha^{-1})\right]^{1/3} \quad \text{for } m \geq 2 \qquad (27)$$

With the increase of α, the critical radius R_m experiences a slow decrease and a successive increase. The value of R_m remains finite, which is different from the results for spheres.

V. Lamellar Domains

With the lowest spatial symmetry, isolated lamellar domains are energetically favorable in the case of strong attraction ($\alpha > 0.846$). In this section, we investigate the stability of lamellae with respect to shape fluctuations. The length, height, and width of a lamellar domain are denoted by L_1 ($\gg 1$), L_2 ($\gg 1$), and h, respectively. Two small shape fluctuations, $s(x, y)$ and $s'(x, y)$, are introduced on boundaries $z = 0$ and $z = h$, respectively. The domain volume changes from $V_{d,0} = L_1L_2h$ to

$$V_d = \int_{-L/2}^{L/2} dx \int_{-L/2}^{L/2} dy \int_{s(x,y)}^{h+s'(x,y)} dz$$
$$= V_{d,0} + \int_{-\infty}^{\infty} dx \int_{-\infty}^{\infty} dy[s'(x, y) - s(x, y)] \qquad (28)$$

For convenience, we introduce two-dimensional vectors, $\vec{r}_\perp = x\hat{e}_x + y\hat{e}_y$ in the real space and $\vec{q}_\perp = q_x\hat{e}_x + q_y\hat{e}_y$ in the Fourier space. To satisfy the constant-volume constraint for stable domains, the shape fluctuation around $z = 0$ is expanded as

$$s(\vec{r}_\perp) = \frac{1}{L_1L_2}\sum_{\vec{q}_\perp\neq 0} s_{\vec{q}_\perp} e^{i\vec{q}_\perp\cdot\vec{r}_\perp} \qquad (29)$$

where $s_{\vec{q}_\perp} = \int d\vec{r}_\perp s(\vec{r}_\perp) \exp(-i\vec{q}_\perp\cdot\vec{r}_\perp)$ is the Fourier transform of $s(\vec{r}_\perp)$. The same expansion is applied to the shape fluctuation, $s'(\vec{r}_\perp)$, around $z = h$. The successive expansion used for spheres and cylinders is unnecessary for lamella, since only linear terms of shape fluctuations appear in eq 28.

With respect to the shape fluctuations on two boundaries, the quadratic truncation of the surface area change is

$$\delta S_d \approx \int_{-L_1/2}^{L_1/2} dx \int_{-L_2/2}^{L_2/2} dy \left[\sqrt{1 + |\nabla_{\vec{r}_\perp} s(\vec{r}_\perp)|^2} + \sqrt{1 + |\nabla_{\vec{r}_\perp} s'(\vec{r}_\perp)|^2} - 2\right]$$
$$\approx \frac{1}{2}\int_{-\infty}^{\infty} dx \int_{-\infty}^{\infty} dy \left[|\nabla_{\vec{r}_\perp} s(\vec{r}_\perp)|^2 + |\nabla_{\vec{r}_\perp} s'(\vec{r}_\perp)|^2\right] \qquad (30)$$

where $\nabla_{\vec{r}_\perp} = \partial_x\hat{e}_x + \partial_y\hat{e}_y$ is the gradient for the two-dimensional vector $\vec{r}_\perp$. Substituting the expansion forms of $s(\vec{r}_\perp)$ and $s'(\vec{r}_\perp)$ into the equation above, we obtain the surface free energy variation

$$\delta F_S = \gamma\delta S_d = \frac{\gamma}{2L_1L_2}\sum_{\vec{q}_\perp\neq 0} q^2{}_\perp\left[|s_{\vec{q}_\perp}|^2 + |s'_{\vec{q}_\perp}|^2\right] \qquad (31)$$

The variation of the intradomain repulsion is similarly expanded to quadratic terms, resulting in

$$\delta F_Y^{(1)} = \frac{\rho_1^2}{2}\int d\vec{r}_{\perp 1}\, d\vec{r}_{\perp 2} u_Y(r_{\perp 12})[s_1s_2 + s'_1s'_2 - s_1^2 - (s'_1)^2] +$$
$$\frac{\rho_1^2}{2}\int d\vec{r}_{\perp 1}\, d\vec{r}_{\perp 2} u_Y([r^2{}_{\perp 12} + h^2]^{1/2})[s_1^2 + (s'_1)^2 - s_1s'_2 - s'_1s_2] \qquad (32)$$

where $r_{\perp 12} = |\vec{r}_{\perp 1} - \vec{r}_{\perp 2}|$, and the subscripts for the shape fluctuations s and s' denote the associated vector variables, e.g., $s_1 \equiv s(\vec{r}_{\perp 1})$. Using the expansion forms for two shape fluctuations, $\delta F_Y^{(1)}$ is diagonalized in the Fourier space as

$$\delta F_{\mathrm{Y}}^{(1)} = \frac{\pi\rho_1^2 A}{2L_1L_2}\sum_{\vec{q}_\perp\neq 0}(|s_{\vec{q}_\perp}|^2 + |s'_{\vec{q}_\perp}|^2)[g_0(h) + g_{q_\perp}(0) - g_0(0)] - g_{q_\perp}(h)[s_{\vec{q}_\perp}(s'_{\vec{q}_\perp})^* + (s_{\vec{q}_\perp})^* s'_{\vec{q}_\perp}] \quad (33)$$

where $g_{q_\perp}(z)$ arises from the Fourier transform of the Yukawa potential, $\pi A g_{q_\perp}(z) = \int d\vec{r}_\perp u_{\mathrm{Y}}([r_\perp^2 + z^2]^{1/2}) \exp(i\vec{q}_\perp\cdot\vec{r}_\perp)$. In the low-density limit, the free energy variation δF for a lamellar domain is the sum of eqs 31 and 33.

To clearly demonstrate shape fluctuations, we consider single-frequency modes, i.e., $s(\vec{r}_\perp) = s_0\cos(\vec{k}_\perp\cdot\vec{r}_\perp)$, and $s'(\vec{r}_\perp) = s'_0\cos(\vec{k}_\perp\cdot\vec{r}_\perp + \phi)$, where s_0 and s'_0 are amplitudes, $\vec{k}_\perp$ is a 2D wavevector, and ϕ is the phase difference. The free energy variation is simplified to a harmonic form, $\delta F = C(\omega_+ s_+^2 + \omega_- s_-^2)$, where $C = \pi\rho_1^2 A L_1 L_2/4$ is a width-independent constant. The eigenfrequencies corresponding to two eigenmodes, $s_\pm = (s_0 \pm s'_0)/2$, are

$$\omega_\pm = \alpha k^2{}_\perp - g_0(0) + g_{k_\perp}(0) + g_0(h) \mp g_{k_\perp}(h)\cos\phi \quad (34)$$

respectively. Since these two eigenfrequencies can be made equivalent by adjusting the phase difference ϕ, we assume the amplitudes of two shape fluctuations are the same, $s_0 = s'_0$. The eigenmode s_- vanishes, and the free energy variation becomes $\delta F = C\omega_+ s_0^2$. In addition, we consider two limiting phase differences, in-phase ($\phi = 0$) and out-phase ($\phi = \pi$), as shown in Figure 5. The phase differences with an intermediate value can be treated as a superposition of these two limits. For the in-phase shape fluctuation, the eigenfrequency for mode s_+ is asymptotically expanded as

$$\omega_+(\phi = 0) \approx k^2{}_\perp[\alpha + (1+h)\mathrm{e}^{-h} - 1] + \frac{k^4{}_\perp}{4}[3 - \mathrm{e}^{-\mathrm{h}}(h^2 + 3h + 3)] + O(k^6{}_\perp) \quad (35)$$

in the long wavelength limit ($k_\perp \to 0$). As shown in ref 20, the first term on the right-hand side of eq 35 becomes negative when the lamellar width is larger than the equilibrium value h_{eq}. The long wavelength in-phase shape fluctuations thus can irreversibly distort nonequilibrium lamellar domains with $h > h_{\mathrm{eq}}$ and form disordered lamellar phases such as labyrinths.[1,2] For equilibrium lamellae, in-phase fluctuations are equivalent to bending modes in the elasticity theories[26,35,36], since $\omega_+ \propto k_\perp^4$ in the leading order. The eigenfrequency ω_+ ($\phi = 0$) for equilibrium lamellae is plotted in Figure 6 as a function of $k_\perp$ in a wide range. Since ω_+ ($\phi = 0$) quickly increases with $k_\perp$, long-wavelength modes are preferred for in-phase fluctuations with the same amplitudes. As shown in Figure 5, out-phase shape fluctuations are equivalent to width fluctuations and can form cylinders if the amplitude is large. In the long-wavelength limit, the eigenfrequency is asymptotically given by

$$\omega_+(\phi = \pi) = 4\,\mathrm{e}^{-\mathrm{h}} + k^2{}_\perp[\alpha - 1 - (1+h)\mathrm{e}^{-\mathrm{h}}] + O(k^4{}_\perp) \quad (36)$$

indicating that lamellae can resist out-phase shape fluctuations, since $\omega_+ > 0$. As a comparison with in-phase fluctuations, we plot ω_+ ($\phi = \pi$) in Figure 6 for equilibrium lamellae. The minimum value of ω_+ ($\phi = \pi$) appears at a finite wavenumber $k_{\perp m}$, implying the largest out-phase fluctuations.[33] The reduced optimal wavenumber $k_{\perp m}h_{\mathrm{eq}}$ is plotted in Figure 7, which demonstrates that $k_{\perp m}^{-1}$ is in the same order as the equilibrium width h_{eq} in a broad range of α. Sizes of cylinders induced by out-phase fluctuations are thus expected to be close to original lamellar widths, consistent with the study of the stripe−bubble transformation in two-dimensional lipid systems.[33] However, this shape transformation is not spontaneous, and an energy barrier $\delta F(k_{\perp m})$ is required to be conquered by thermal fluctuations.

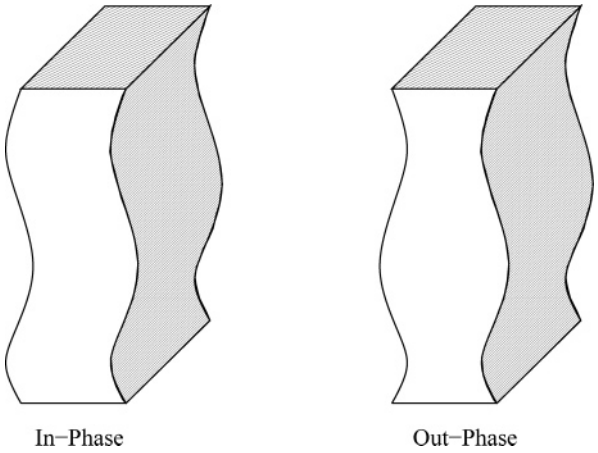

Figure 5. Two important shape fluctuation modes for lamellar domains. The left is an in-phase fluctuation mode ($\phi = 0$), and the right is an out-phase fluctuation mode ($\phi = \pi$).

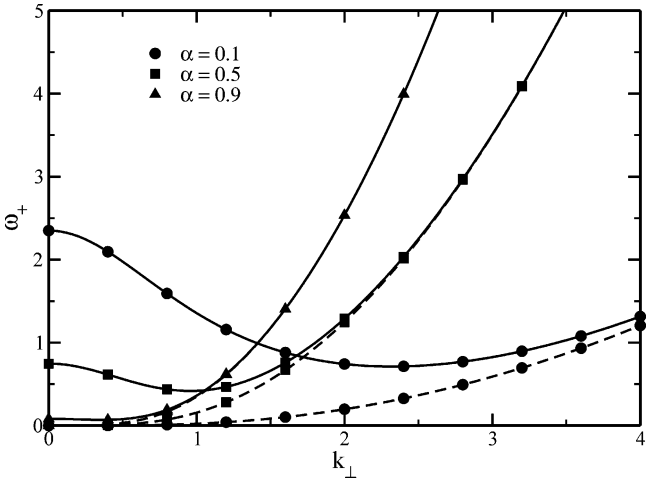

Figure 6. The eigenfrequency ω_+ as a function of wavenumber $k_\perp$ for equilibrium lamellar domains ($h = h_{\mathrm{eq}}$). The dashed lines correspond to in-phase fluctuations ($\phi = 0$), and the solid lines correspond to out-phase fluctuations ($\phi = \pi$). The values of the control parameter α are as follows: $\alpha = 0.1$ for lines with circles, $\alpha = 0.5$ for lines with squares, and $\alpha = 0.9$ for lines with up triangles.

In addition to the phenomena discussed in the previous section, shape fluctuations of cylinders can also occur along the azimuthal axis. The azimuthal fluctuations can be considered as superpositions of two fundamental modes. For the first mode, the center of the circular cross-section fluctuates around the azimuthal axis of the original cylinder, whereas the radius of the circular cross-section is the same as the original value. This mode is similar to the in-phase fluctuation for lamellae. For the second mode, the circular centers are kept in a straight line, whereas the radius of the circular cross-section fluctuates periodically along the azimuthal axis. This mode is similar to the out-phase fluctuations for lamellae. Because of the spatial similarities, we would expect that the first type of shape fluctuations can be realized with less energy costs than the second type. However, to obtain quantitative results of these two modes, detailed calculations are needed in the future.

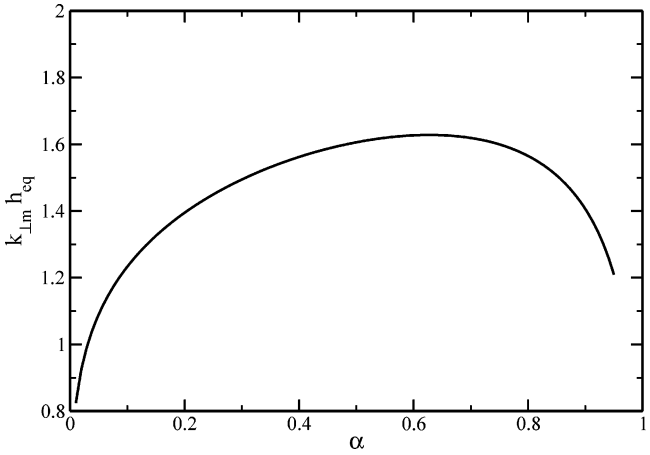

Figure 7. The dimensionless optimal wavenumber $k_{\perp m}h_{eq}$ as a function of the control parameter α. Given by the minimum of the eigenfrequency $\omega_+(k_{\perp m})$ for equilibrium lamellae (see Figure 6), $k_{\perp m}$ indicates the wavenumber of the out-phase fluctuation with the largest amplitude.

VI. Discussions

In charged colloidal suspensions with competing short-range attraction and long-range Yukawa repulsion, three-dimensional domain patterns can be self assembled. Following an early investigation of ground-state shapes,[20] in this paper we analyze the stability of isolated spherical, cylindrical, and lamellar domains with respect to shape fluctuations, which effectively describe entropic effects at low temperatures. Our stability analysis adopts the simplified continuum model and follows closely the approach introduced by Deutch and Low.[27] Under the constraint of constant volume for stable domains, shape fluctuations are expanded in successive orders and used to calculate the free energy variation δF within the quadratic approximation. The sign of δF determines the stability of domains: The reference shape can be recovered for $\delta F > 0$, whereas a spontaneous distortion occurs for $\delta F < 0$. On the basis of this criterion, spherical, cylindrical, and lamellar domains with equilibrium sizes are stable with respect to small shape fluctuations in the quadratic approximation. In addition, the domain stability decreases as the spatial symmetry decreases. Spherical domains have the highest spatial symmetry. For $\alpha > 0.5$, all the spherical domains are stable with respect to shape fluctuations, and the transformation from spheres to other shapes are not spontaneous. With the lowest spatial symmetry, lamellar domains whose widths are larger than the equilibrium value h_{eq} are unstable with respect to in-phase shape fluctuations in the long wavelength limit. Instead of ordered one-dimensional lattice, disordered labyrinths composed of lamellae are often observed in experiments and simulations.[1,2] Between limiting cases of spheres and lamellae, critically stable sizes of cylindrical domains are finite but larger than the equilibrium value with respect to shape fluctuations about the radius. Another interesting result of this paper is that out-phase fluctuations can transform lamellar domains to cylinders with similar sizes through an activation process, consistent with the study of two-dimensional lipids.[33]

In this paper, we focus on the low-temperature and low-density regime, where each domain can be treated as an isolated system. With the increase of temperature, shape fluctuations with large amplitudes become important. Higher-order free energy variations are required to improve the quadratic approximation in our analysis. For finite volume fraction, the variation of interdomain repulsions has to be included. When the system approaches the homogeneous state, the density change from colloidal domains to surrounding environments becomes smooth, and sharp boundaries are hard to define. Accordingly, thermal fluctuations are better described by density fluctuations, and the simple continuum model in this paper has to be modified.[9,10] For example, the transition between domains and the homogeneous phase has recently been predicted using density fluctuations in the Hartree approximation.[17] Dynamics of charged colloids is also important in predicting the phase behaviors of domain patterns. In the diffusion-limited process,[37] domains with fractal structures can be formed. Computer simulations demonstrate domains with loose structures.[38] Nonequilibrium glassy states of domains with local structural arrest can be found in quenching processes. The cluster glass transition has been studied in charged colloids within the framework of mode-coupling theory,[16,17,21,22,39−41] and further theoretical efforts are needed to include hopping processes.

Acknowledgment. This work is supported by the NSF Career Award (Che-0093210) and the Camille Dreyfus Teacher-Scholar Award. We dedicate this paper to Professor Irwin Oppenheim with admiration. His work on the mode-coupling theory has influenced many of our papers.

Appendix A: Intradomain Repulsion Variation for Spherical Domains

As shown in eq 12, the quadratic truncation of $\delta F_Y^{(1)}$ for a spherical domain is a sum of two integrals, which will be denoted by W_A and W_B for convenience. In this appendix, we use the spherical harmonic expansion to explicitly calculate W_A and W_B.

The first step is to expand the Yukawa potential $u_Y(r_{12})$ by spherical harmonics. An arbitrary function $g(t)$ with $t \in [-1, 1]$ can be expanded in the basis of Legendre polynomials $P_l(t)$ as

$$g(t) = \sum_{l=0}^{\infty} \frac{2l+1}{2} g_l P_l(t) \tag{A1}$$

where the coefficient g_l is defined by $g_l = \int_{-1}^{1} dt\, g(t)\, P_l(t)$. Since the explicit form of r_{12} is $r_{12} = (r_1^2 + r_2^2 - 2r_1r_2 \cos\chi)^{1/2}$ where χ is the angle between vectors $\vec{r}_1$ and $\vec{r}_2$ and $\cos\chi = \cos\theta_1 \cos\theta_2 + \sin\theta_1 \sin\theta_2 \cos(\phi_1 - \phi_2)$, and we use eq A1 to expand $u_Y(r_{12})$ in the basis of $P_l(\cos\chi)$ as

$$u_Y(r_{12}) = \sum_{l=0}^{\infty} \frac{2l+1}{2} A g_l(r_1, r_2) P_l(\cos\chi) \tag{A2}$$

where the coefficient $g_l(r_1, r_2)$ is given by

$$g_l(r_1, r_2) = A^{-1} \int_0^{\pi} \sin\chi\, u_Y(\sqrt{r^2_1 + r^2_2 - 2r_1r_2\cos\chi}) P_l(\cos\chi) d\chi \tag{A3}$$

Following the additional theorem for Legendre polynomials

$$P_l(\cos\chi) = \frac{4\pi}{2l+1} \sum_{m=-l}^{l} Y_{lm}(\Omega_1) Y^*_{lm}(\Omega_2) \tag{A4}$$

we further simplify $u_Y(r_{12})$ to be

$$u_Y(r_{12}) = 2\pi A \sum_{l=0}^{\infty} \sum_{m=-l}^{l} g_l(r_1, r_2) Y_{lm}(\Omega_1) Y^*_{lm}(\Omega_2) \tag{A5}$$

Using the expansion forms for the shape fluctuation $\delta R_0(\Omega)$ and the Yukawa potential $u_Y(r_{12})$, the first integral on the right-hand side of eq 12 is derived as

$$W_A = \frac{R^4\rho_1^2}{2}\oint d\Omega_1 \oint d\Omega_2\, \delta R_0(\Omega_1)\, \delta R_0(\Omega_2) u_Y(|R\hat{e}_{r_1} - R\hat{e}_{r_2}|)$$

$$= \pi R^4\rho_1^2 A \oint d\Omega_1 \oint d\Omega_2 [\sum_{l_1=1}^{\infty}\sum_{m_1=-l_1}^{l_1} c^*_{l_1m_1} Y^*_{l_1m_1}(\Omega_1)] \times$$

$$[\sum_{l_2=1}^{\infty}\sum_{m_2=-l_2}^{l_2} c_{l_2m_2} Y_{l_2m_2}(\Omega_2)][\sum_{l=0}^{\infty}\sum_{m=-l}^{l} g_l(R,R) Y_{lm}(\Omega_1) Y^*_{lm}(\Omega_2)]$$

$$= \pi R^4\rho_1^2 A \sum_{l_1,l_2=1}^{\infty}\sum_{l=0}^{\infty}\sum_{m_1,m_2,m} c^*_{l_1m_1} u_l(R,R) c_{l_2m_2} g_l(R,R) \delta_{l_1,l}\delta_{m,m_1}\delta_{l_2,l}\delta_{m,m_2}$$

$$= \pi R^4\rho_1^2 A \sum_{l=1}^{\infty}\sum_{m=-l}^{l} g_l(R,R)|c_{lm}|^2 \qquad \text{(A6)}$$

Rearranging the second integral W_B to be

$$W_B = \frac{R^2\rho_1^2}{2}\oint d\Omega_2\, \delta R^2{}_0(\Omega_2) w_B(\Omega_2) \qquad \text{(A7)}$$

where

$$w_B(\Omega_2) = \oint d\Omega_1 \int_0^R dr_1 r^2{}_1\, \partial_{r_2} u_Y(|\vec{r}_1 - R\hat{e}_{r_2}|) \qquad \text{(A8)}$$

we can straightforwardly use the spherical harmonic expansion to prove that $\omega_B(\Omega_2)$ is independent of Ω_2. A specific set of solid angles, $\Omega_2 = \{\theta_2 = \pi/2, \phi_2 = 0\}$, is introduced to simplify w_B, resulting in

$$w_B = \int_{-R}^{R} dz_1 \int_{-\sqrt{R^2-z_1^2}}^{\sqrt{R^2-z_1^2}} dy_1 \int_{-\sqrt{R^2-z_1^2-y_1^2}}^{\sqrt{R^2-z_1^2-y_1^2}} dx_1\, \partial_{x_2} u_Y(\sqrt{(R-x_1)^2 + y_1^2 + z_1^2})$$

$$= -2\pi \int_0^R d\rho\rho [u_Y(\sqrt{2R^2 - 2R\sqrt{R^2-\rho^2}}) - u_Y(\sqrt{2R^2 + 2R\sqrt{R^2-\rho^2}})]$$

$$= -2\pi R^2 \int_0^{\pi} d\theta \sin\theta \cos\theta u_Y(\sqrt{2R^2(1-\cos\theta)})$$

$$= -2\pi R^2 A g_1(R,R) \qquad \text{(A9)}$$

The second integral on the right-hand side of eq 12 is given by

$$W_B = -\pi R^4\rho_1^2 A g_1(R,R)\sum_{l=1}^{\infty}\sum_{m=-l}^{l}|c_{lm}|^2 \qquad \text{(A10)}$$

As a result, we obtain the spherical harmonic expansion of $\delta F_Y^{(1)}$ in eq 13.

References and Notes

(1) Möhwald, H. *Annu. Rev. Phys. Chem.* **1990**, *41*, 441.
(2) Seul, M.; Andelman, D. *Science* **1995**, *267*, 476.
(3) Shiloach, A.; Blankschtein, D. *Langmuir* **1998**, *14*, 7166.
(4) Tsonchev, S.; Schatz, G. C.; Ranter, M. A. *J. Phys. Chem. B* **2004**, *108*, 8817.
(5) Sear, R. P.; Chung, S. W.; Markovich, G.; Gelbart, W. M.; Heath, J. R. *Phys. Rev. E* **1999**, *59*, R6255.
(6) Kindt, J. T.; Gelbart, W. M. *J. Chem. Phys.* **2001**, *114*, 1432.
(7) Lipowsky, R. *Nature (London)* **1991**, *349*, 475.
(8) Ayton, G.; Voth, G. A. *Biophys. J.* **2002**, *83*, 3357.
(9) Leibler, L. *Macromolecules* **1980**, *13*, 1602.
(10) Ohta, T.; Kawasaki, K. *Macromolecules* **1986**, *19*, 2621.
(11) Fredrickson, G. H.; Helfand, E. *J. Chem. Phys.* **1987**, *87*, 697.
(12) Blankschtein, D.; Thurston, G. M.; Benedek, G. B. *Phys. Rev. Lett.* **1985**, *54*, 955.
(13) Widom, B.; Dawson, K. A.; Lipkin, M. D. *Phys. A* **1986**, *140*, 26.
(14) Dawson, K. A. *Phys. Rev. A* **1987**, *36*, 3383.
(15) McConnell, H. M. *Annu. Rev. Phys. Chem.* **1991**, *42*, 171.
(16) Schmalian, J.; Wolynes, P. G. *Phys. Rev. Lett.* **2000**, *85*, 836.
(17) Wu, S. W.; Westfahl, H.; Schmalian, J.; Wolynes, P. G. *Chem. Phys. Lett.* **2002**, *359*, 1.
(18) Maibaum, L.; Dinner, A. R.; Chandler, D. *J. Phys. Chem. B* **2004**, *108*, 6778.
(19) Stoycheva, A. D.; Singer, S. J. *Phys. Rev. Lett.* **2000**, *84*, 4657.
(20) Wu, J. L.; Cao, J. S. To be submitted.
(21) Wu, J. L.; Liu, Y.; Chen, W. R.; Cao, J. S.; Chen, S. H. *Phys. Rev. E* **2004**, *70*, 050401.
(22) Sciortino, F.; Mossa, S.; Zaccarelli, E.; Tartaglia, P. *Phys. Rev. Lett.* **2004**, *93*, 055701.
(23) Verwey, E. J. W.; Overbeek, J. Th. G. *Theory of the Stability of Lyophobic Colloids*; Elsevier: Amsterdam, 1948.
(24) Wu, C.; Chen, S. H. *J. Chem. Phys.* **1987**, *87*, 6199.
(25) McConnell, H. M. *J. Phys. Chem.* **1990**, *94*, 4728.
(26) de Koker, R.; Jiang, W. N.; McConnell, H. M. *J. Phys. Chem.* **1995**, *99*, 6251.
(27) Deutch, J. M.; Low, F. E. *J. Phys. Chem.* **1992**, *96*, 7097.
(28) Mayer, M. A.; Vanderlick, T. K. *J. Chem. Phys.* **1994**, *100*, 8399.
(29) Ng, K. O.; Vanderbilt, D. *Phys. Rev. B* **1995**, *52*, 2177.
(30) Laradji, M.; Shi, A. C.; Noolandi, J.; Desai, R. C. *Macromolecules* **1997**, *30*, 3242.
(31) Kashuba, A. B.; Pokrovsky, V. L. *Phys. Rev. B* **1993**, *48*, 10335.
(32) Muratov, C. B. *Phys. Rev. E* **2002**, *66*, 066108.
(33) Deutsch, A.; Safran, S. A. *Phys. Rev. E* **1996**, *54*, 3906.
(34) Watson, G. N. *A Treatise on the Theory of Bessel Functions*; Cambridge University Press: New York, 1944.
(35) Grinstein, G.; Pelcovits, R. A. *Phys. Rev. A* **1982**, *26*, 915.
(36) Landau, L. D.; Lifshitz, E. M. *Theory of Elasticity*; Pergamon Press: New York, 1970.
(37) Witten, T. A.; Sander, L. M. *Phys. Rev. Lett.* **1981**, *47*, 1400.
(38) Gutman, L.; Yang, L.; Cao, J. S. In preparation.
(39) Liu, C. Z. W.; Oppenheim, I. *Phys. A* **1997**, *247*, 183.
(40) Mauro, M.; Oppenheim, I. *Phys. A* **1999**, *265*, 520.
(41) Cates, M. E.; Fuchs, M.; Kroy, K.; Poon, W. C. K.; Puertas, A. M. *J. Phys.: Condens. Matter* **2004**, *16*, S4861.